APPROXIMATE ANALYTIC INVESTIGATION OF A TURBULENT GRADIENT BOUNDARY LAYER

V. T. Movchan

UDC 532.526

Numerical integration of the turbulent boundary-layer equations [1-12] aided the estimation of the possibilities of many semiempirical hypotheses, and the refinement of the limits of applicability of a number of empirical dependences and coefficients. Analysis of the numerical computations of many authors shows that the computed curves deviated noticeably from the experimental dependences [2-6, 11-14] for an abrupt change in the pressure gradient. An especially significant deviation is observed upon approaching the separation zone, which is usually explained by not having taken account of the normal Reynolds stresses and the three-dimensionality of the flow [2, 3, 11, 13]. Not taking into account the influence of the pressure gradient and small Reynolds numbers on the empirical coefficients used in algebraic and differential models [2, 3, 10, 11] plays a definite role. The correction to the gradient was initially taken into account in the Van Driest coefficient [2, 3, 5, 11, 12]. It turns out that the approximate Cebecci [2, 12] and Case [5] formulas for taking account of the pressure gradient influence on the Van Driest coefficient yield quite distinct numerical values. It is known that the influence of the pressure gradient is manifested considerably more weakly in the near-wall region than in the exterior [3, 11, 16]. Hence, the influence of the pressure gradient on the coefficient of the outer domain will be most substantial. Not only the present investigation indicates this. The numerical experiment in [14] on materials from the Stanford conference [15] showed that the mixing path length l, referred to the boundary layer thickness δ, which is assumed constant in a normal section of the outer region according to the Prandtl–Escudier model, changes in a gradient flow. It depends on the pressure gradient, and for an unfavorable gradient decreases as it grows from the value 0.09 in gradient-free flows to the value 0.045 in near-wall sections. The constancy of the quantity l/δ in the computation resulted in a systematic exaggeration of the surface friction coefficient c_f and a reduction in the values of the form-parameter H, and did not permit prediction of the possible flow separation [4]. A still greater diminution in the l/δ value as the unfavorable pressure gradient grew is shown in [6] (from 0.089 to 0.0125). In a number of investigations corrections for the gradient or small Reynolds numbers were introduced in individual coefficients [2-6, 11, 12, 14]. However, no complete investigation of the influence of the pressure gradient and small Reynolds numbers has apparently been performed. As a rule, the influence of the pressure gradient or of small Reynolds numbers is estimated on the basis of comparing values of the surface friction coefficient c_f, the form-parameter H, and the thickness of the momentum loss δ^{**} with tests. It is hence of indubitable interest to use approximations for the velocity profiles in these cases. Moreover, a two-layer scheme is realized in a numerical computation with algebraic models: Different formulas for the turbulent viscosity coefficient will be taken in the near wall and outer regions. The solutions are joined at either a previously selected ordinate, or it is found during solution of the problem by equating values of the turbulent viscosity coefficient from the near-wall and outer regions [2, 3, 5, 11, 12]. However, the problem of matching the turbulent viscosity coefficient turns out to be incorrect [14]. The ordinate of the juncture point should decrease as the positive pressure gradient grows, but it is either constant or still increases [14]. Therefore, there is a need for further investigations and refinements of the algebraic models. And even more so since preference is given to algebraic models for a numerical computation in engineering practice [11]. Moreover, algebraic models [7, 10] are used initially in attempts at a numerical computation of a three-dimensional turbulent boundary layer.

1. The purpose of this paper is to refine a single formula for the turbulent viscosity coefficient for the whole boundary layer [17-19], to construct approximate expressions for the velocity profiles taking positive and negative pressure gradients into account, to study the influence of the pressure gradient on the empirical coefficients of the zones and regions of the turbulent boundary layer. To achieve these ends, an approximately analytic approach is used. A reasonable combination of numerical experiments and computations with approximately analytic solutions will permit significant expansion of the possibilities of investigations. Taken as the basis for this research is a single semiempirical formula for the turbulent viscosity coefficient for the whole boundary layer, of the form [17]

Kiev. Translated from Zhurnal Prikladnoi Mekhaniki i Tekhnicheskoi Fiziki, No. 3, pp. 102-111, May-June, 1982. Original article submitted March 23, 1981.

0021-8944/82/2303-0402$07.50 © 1982 Plenum Publishing Corporation

$$\varepsilon = \rho\varkappa\Delta v_* \gamma \operatorname{th} l \sqrt{\tau_+}/\varkappa\Delta, \tag{1.1}$$

where ε is the turbulent viscosity coefficient; $\varkappa$, an empirical constant; ν, a function of the intermittent coefficient type; v_*, dynamic velocity; Δ, Clauser length parameter; l, mixing path length; δ, boundary layer thickness; τ_0, friction stress in the neighborhood of the wall; τ_W, friction stress on the wall; $\eta = y/\delta$; $\tau_+ = \tau_0/\tau_W$; $\tau_+ = 1 + \Phi\eta$ for a positive pressure gradient; and $\tau_+ = 1/(1 - \Phi\eta)$ for a negative gradient; $\Phi = (\delta/\tau_W)\partial p/\partial x$; p, pressure; and ρ, density. In a stream with acceleration the linear dependence of the tangential stress distribution in the neighborhood of the wall can result in negative values for $\Phi < -1$, and consequently, in this case the reduced nonlinear dependence from [18] can be used. The outer boundary layer domain and the potential flow are separated by a thin sublayer through which turbulized and unturbulized fluid volume exchange occurs because of viscous forces. Near the wall the turbulence is practically completely continuous in time, but becomes all the more intermittent at the outer boundary of the boundary layer. Selected as the measure of intermittency is the ratio between the time interval during which turbulent motion is observed and the total time interval, called the intermittency coefficient. If the behavior of the change in the turbulent viscosity coefficient is traced in the outer region, then it is detected that near the near-wall region it varies quite weakly but starts to diminish rapidly upon approaching the potential flow. Similar behavior of the turbulent viscosity coefficient is observed in wakes and jets. Townsend showed that the computed values of the velocity profiles for the flow of a plane wake can be improved considerably if the effective coefficient of turbulent viscosity were considered as the product of the turbulent viscosity coefficient and the intermittency coefficient. The Townsend assumption is now used in many papers [2, 3, 9, 12] for the approximate taking account of the nature of the flow in jets, wakes, and boundary layers. In this paper, the approximate formulas of Klebanoff and Cevecci [2], linear [17], and that proposed below were used for the coefficient of intermittency. It turns out that the linear formula permits obtaining satisfactory results for the friction stress and velocity defect profiles with constant coefficients for both the positive and the negative pressure gradients [17, 18]. However, a substantial divergence is observed between the computation [19] and experiment [16] for the turbulent viscosity coefficient on a flat plate. The Klebanoff and Cebecci formulas permitted good agreement to be obtained with test for the turbulent viscosity coefficient if the mixing path length in the transverse section is given by several interpolation formulas [19]. In combination with the method of lines, this approach permitted organization of a numerical computation on a flat plate [8, 9]. The computation was also performed on two-layer (viscous sublayer, turbulent core), and continuous models [8, 9]. The formula $\gamma = (1 - \eta)^{1/2}$ permitted obtaining fair agreement between computation and test for the turbulent viscosity coefficient on a flat plate [16] if the known Prandtl formula $l = \mathrm{k}y$ is used for l outside the viscous and transition zones. Taking account of the flow specifics in the viscous and transition zones [3, 11, 16] results in a formula for the mixing path length of the whole boundary layer in this case

$$l = ky \operatorname{th} \frac{\operatorname{sh}^2\left[\varkappa_1 y^+ \left(1 + \varkappa_3 \left| y^+ - 30 \right|\right)\right] \operatorname{th}\left[\operatorname{sh}^2\left(\varkappa_2 y^+\right)\right]}{ky^+ \sqrt{\tau_+}},$$

where $y^+ = yv_*/\nu$, k, $\varkappa_1$, $\varkappa_2$, $\varkappa_3$ are empirical coefficients, and ν is the coefficient of kinematic viscosity. In constructing interpolation formulas for l it is taken into account that the turbulent viscosity coefficient is proportional to y^m in the wall region and m is different in each of the zones [16]. As in [16] also, it is assumed that m = 4 in the viscous sublayer, m = 2 in the transition zone, and m = 1 in the wall law zone. A comparison between computed values of the turbulent viscosity coefficient and experiment on a flat plate indicates totally satisfactory agreement for k = 0.4, $\varkappa_1 = 0.064$, $\varkappa_3 = 0.0125$, $\varkappa_2 = 0.17458$. Linearization of the argument of the function $\sinh^2[y^+\varkappa_1(1 + \varkappa_3 | y^+ - 30|)]$ permits obtaining a simplified formula [19]

$$l = ky \operatorname{th} \frac{\operatorname{sh}^2\left(\varkappa_1 y^+\right) \operatorname{th}\left[\operatorname{sh}^2\left(\varkappa_2 y^+\right)\right]}{ky^+ \sqrt{\tau_+}}, \tag{1.2}$$

which is convenient in that it permits finding approximate solutions for the velocity profiles in the transition and viscous zones. The computed values of the turbulent viscosity coefficient from (1.1) and (1.2) indicate, when compared with experiment [16], an insignificant excess in the computation for $20 < y^+ < 40$. Numerical computations [9] and the reduced modified model permit the conclusion that (1.1) and (1.2) are convenient in application.

2. To clarify the influence of the positive pressure gradient on the velocity profile, and on the zone and region coefficients, approximately analytic solutions were constructed. It was assumed that $\gamma = 1$ in obtaining the approximate solutions in the zones of the near-wall regions. An approximate formula [19]

$$\varepsilon_* = \mu \operatorname{ch}^2(\varkappa_1 y^+), \tag{2.1}$$

was found by the superposition principle from (1.1) and (1.2) for the coefficient of total viscosity in the transition zone, where μ is the coefficient of dynamic viscosity. This last expression permits finding the dependence for the velocity profile in the transition zone for a positive pressure gradient of the form

$$u^+ = \frac{1 + p^+ y^+}{\varkappa_1} \operatorname{th}(\varkappa_1 y^+) - \frac{p^+}{\varkappa_1^2} \ln[\operatorname{ch}(\varkappa_1 y^+)], \qquad u^+ = \frac{u}{v_*},\ p^+ = \frac{\nu}{\rho v_*^3}\frac{\partial p}{\partial x}, \tag{2.2}$$

if the approximation

$$\tau = \tau_w(1 + p^+ y^+). \tag{2.3}$$

is considered valid for the friction stress in the near-wall region. For gradient-free flow, (2.2) goes over into the Rann formula [16, 19, 20, 21]

$$u^+ = (1/\varkappa_1)\operatorname{th}(\varkappa_1 y^+), \tag{2.4}$$

which fairly describes test even for a flow in a tube with $\varkappa_1 = 0.0688$ in the transition and viscous zones. It is known that the turbulent component is neglected in the viscous zone when determining the velocity profile. This profile will be obtained if $\tanh(\varkappa_1 y^+)$ is expanded into series and just one term is used. We arrive at the same result from (2.1) also since $\cosh(\varkappa_1 y^+) \to 1$ as $y^+ \to 0$. Analysis of (2.1), (2.2), and (2.4) permits the conclusion that (2.2) is also applicable in the viscous zone. The profile (2.4) is used in [20] for a flow with positive pressure gradient for $y^+ = 27.5$ and $\varkappa_1 = 0.0688$. However, $\varkappa_1 = 1/14$ is obtained in flow investigations on a flat plate [21]. The nearby value $\varkappa_1 = 0.072$ is found in the numerical experiment in [9]. Moreover, as the unfavorable pressure gradient grows, the thickness of the viscous and transition zones should decrease. Formulas (1.1), (1.2), and (2.4) permit finding such a dependence

$$u^+ = \frac{1}{k}\left[\ln \frac{\sqrt{1 + p^+ y^+} - 1}{\sqrt{1 + p^+ y^+} + 1} + 2\sqrt{1 + p^+ y^+}\right] + C \tag{2.5}$$

in the wall law zone. In the case of a zero pressure gradient (2.5) goes over into the known wall law

$$u^+ = (1/k)\ln y^+ + C. \tag{2.6}$$

The dependence (2.5) seems to be a "generalized wall law" from which two limit "laws" will follow. Indeed, for $\tau_W \gg (y/\rho)\partial p/\partial x$ we arrive at the "wall law" (2.6), and in the case $\tau_W \ll (y/\rho)\partial p/\partial x$ at the "1/2 wall law" [3, 20]:

$$u = (2/k)\sqrt{(y/\rho)\partial p/\partial x} + \text{const}.$$

The velocity profiles (2.2), (2.5), and (2.4), (2.6) permit obtaining the following dependences to evaluate C:

$$C = \frac{1 + p^+ y^+}{\varkappa_1} \operatorname{th}(\varkappa_1 y_*) - \frac{p^+}{\varkappa_1^2} \ln[\operatorname{ch}(\varkappa_1 y_*)] - \frac{1}{k}\left[\ln \frac{\sqrt{1 + p^+ y_*} - 1}{\sqrt{1 + p^+ y_*} + 1} + 2\sqrt{1 + p^+ y_*}\right]; \tag{2.7}$$

$$C = \operatorname{th}(\varkappa_1 y_*)/\varkappa_1 - \ln y_*/k, \tag{2.8}$$

where y_* is the value of y^+ for which the velocity profiles of the transition zone and the wall law merge. For flow in a tube, the velocity profile (2.4) goes smoothly over into (2.6) for $y_* = 27.5$. The value $y_* = 27.5$ permits finding $C = 5.6$ for $k = 0.4$. The flow on a plate assumes that value of y_* that depends on the selection of the values of $\varkappa_1$, k. In turn, the constant C depends on y_*. Analysis of experimental results and empirical values of the constant C indicates a noticeable spread in the numerical values of this quantity [16]. As is known, the reason for the spread is in the selection of values of C by the experiments, which would yield the best agreement between the computed values from (2.6) and their experiments [16]. Two numerical values of C are used in this paper: $C = 4.78$ for $k = 0.4$ according to Klebanoff and Deal [16], and $C = 5.0$ for $k = 0.41$ according to Cowles [15]. It is seen from (2.8) that $C = 4.77$ for $\varkappa_1 = 0.0688$, $y_* = 49$ and $k = 0.4$ while $C = 5.008$ for $k = 0.41$. If $\varkappa_1 = 0.072$, $y_* = 35$ are taken, then $C = 4.821847$ for $k = 0.4$ while $C = 5.038637$ for $k = 0.41$. Therefore, an increase in $\varkappa_1$ from 0.0688 to 0.072 will result in a drop in y_* from 49 to 35. The natural question arises of

how to determine y_* in the case of a positive pressure gradient and which of the two versions to use. For this purpose, the quantity

$$\alpha_0 = \mathrm{sh}^2(\varkappa_1 y_*)\Big/\left(k y_* \sqrt{1 + p^+ y_*}\right), \tag{2.9}$$

was considered, which was assumed constant and equal to its value for a zero gradient. In other words, (2.9) was used as an equation to find y_*. For a zero pressure gradient and for $\varkappa_1 = 0.0688$, $y_* = 49$, $k = 0.4$ we find $\alpha_0 = 10.7856$, while for $\varkappa_1 = 0.072$, $y_* = 35$, $k = 0.4$ we have $\alpha_0 = 2.723$. Computations and comparisons with experiments [15] showed that the velocity profiles from the zone of the wall law are barely responsive to which of the two values found for α_0 is taken. For a zero pressure gradient, the preference can be given to $\varkappa_1 = 0.072$ in the transition and viscous zones, which means $\alpha_0 = 2.723$. In the case of a flow with positive pressure gradient, the coefficients k, $\varkappa_1$, and $\varkappa_2$ experience the influence of the gradient [2, 5, 12, 22]. Careful analysis of the computations by the formulas presented and their comparison with experimental results [15, 23] and other computations [5, 12] permitted obtaining dependences for the coefficients k, $\varkappa_1$, and $\varkappa_2$ under conditions of a positive pressure gradient:

$$k = 0{,}4 + 0.182275(1 + p^+)(1 - e^{-0{,}32068\beta}); \tag{2.10}$$

$$\varkappa_1 = \varkappa_{10}\varkappa_{1R}\left\{\left[1 + 30.179p^+\left(1 - e^{-0{,}009528\beta}\right)\right] f_1(p^+) + \sqrt[4]{1 + 120.716p^+}\, f_2(p^+)\right\}; \tag{2.11}$$

$$\varkappa_2 = \varkappa_{20}(1 + 30{,}178p^+), \tag{2.12}$$

where $f_1(p^+) = \frac{1}{8}\frac{0{,}007 - p^+}{|0{,}007 - p^+|} + \frac{3}{32}\frac{0{,}04 - p^+}{|0{,}04 - p^+|} + \frac{17}{32}$; $\beta = \frac{\delta^*}{\tau_w}\frac{\partial p}{\partial x}$; $f_2(p^+) = 1 - f_1(p^+)$; $\varkappa_{10} = 0{,}072$; $\varkappa_{20} = 0{,}223$; $\varkappa_{1R}$ is the correction for small Reynolds numbers equal to $\varkappa_{1R} = 1 + 0.01(1 - e^{-14/(1+z^2)})$, $z = 10^{-3}R^{**}$, $R^{**} = \delta^* u_H/\nu$, u_H is the external flow velocity, δ^* is the displacement thickness. A comparison between the computed values of u^+ (dashed line) by using the formulas (2.2), (2.5), (2.7), (2.9)-(2.12) and the experimental results (points) of F. Clauser (id. 2200, x = 11) – a, A. Perry (id. 2900, x = 12.5) – b, W. Newman (id. 3500, x = 2.759) – c [15] is presented in Fig. 1. Also shown there is the wall law (solid line) (2.6) for k = 0.41 and C = 5.0 [15]. As should have been expected, in the case of small values of y^+ very satisfactory agreement of the computed values using (2.5) and (2.6) is observed with the experimental data. Hence, for small values of y^+, for practical purposes (2.6) with the constant coefficients C and k can be used. As the values of y^+ grow, the computed values of u^+ start to deviate from the experimental. The numerical values from (2.6) start to deviate first.

It is known that the velocity defect law is valid in the outer region and an intermediate zone of overlap of the velocity defect and wall laws exists [3, 11, 16]. To obtain approximate dependences for the velocity profiles in the velocity defect and overlap zones, the methodology of [17, 18] was used and $(1 - \eta)^{1/2}$ was first expanded into a series with two terms retained. The following formulas were found:

$$u^- = \frac{1}{k}\left[\ln\eta - 2\ln\left(\sqrt{1 + \Phi\eta} + 1\right) + (2\Phi^2 + 2\Phi + 1)\frac{\sqrt{1 + \Phi\eta}}{\Phi^2} - \frac{\Phi + 1}{3\Phi^2}(1 + \Phi\eta)^{\frac{3}{2}}\right] - \frac{2\Phi}{\varkappa\Delta_1}\left(\frac{\eta^{n+1} - 1}{n + 1} - 0{,}5\frac{\eta^{n+2} - 1}{n + 2}\right) + R_1 \text{ at } \eta \leqslant \eta_1; \tag{2.13}$$

$$u^- = \frac{1}{\varkappa\Delta_1}\left[\eta - 1 + \frac{1 + 2\Phi}{4}(\eta^2 - 1) - \frac{\Phi + 1}{6}(\eta^3 - 1) - (2 + \Phi)\left(\frac{\eta^{n+1} - 1}{n + 1} - 0{,}5\frac{\eta^{n+2} - 1}{n + 2}\right)\right] \text{ at } \eta \geqslant \eta_1, \tag{2.14}$$

where

$$u^- = \frac{u - u_H}{v_*};\ R_1 = \frac{1}{k}\left[-\ln\eta_1 + 2\ln\left(\sqrt{1 + \Phi\eta_1} + 1\right) - (2\Phi^2 + 2\Phi + 1)\frac{\sqrt{1 + \Phi\eta_1}}{\Phi^2} + \frac{\Phi + 1}{3\Phi^2}(1 + \Phi\eta_1)^{\frac{3}{2}}\right] + \frac{1}{\varkappa\Delta_1}\left[\eta_1 - 1 + \frac{1 + 2\Phi}{4}(\eta_1^2 - 1) - \frac{(1 + \Phi)}{6}(\eta_1^3 - 1)\right];$$

$$n = -2{,}5 - \frac{2 + \Phi}{4F} + \sqrt{\left(2{,}5 + \frac{2 + \Phi}{4F}\right)^2 - 6 - \frac{2(2 + \Phi)}{F}};\ \Delta_1 = \frac{\Delta}{\delta};$$

$$F = \varkappa\Delta_1^2 + \frac{\varkappa\Delta_1}{k}F_1 + F_2;\ F_1 = -\frac{2}{\Phi}\sqrt{1 + \Phi\eta_1} + (2\Phi^2 + 2\Phi + 1) \times \frac{2 - \Phi\eta_1}{3\Phi^3}\sqrt{1 + \Phi\eta_1} - (1 + \Phi)\frac{2 - 3\Phi\eta_1}{15\Phi^3}(1 + \Phi\eta_1)^{\frac{3}{2}} + 2\frac{5\Phi^2 - 9\Phi - 4}{15\Phi^3};$$

$$F_2 = 0{,}5\eta_1^2 + \frac{1 + 2\Phi}{6}\eta_1^3 - \frac{\Phi + 1}{4}\eta_1^4 - \frac{5}{24}\Phi - \frac{13}{24};$$

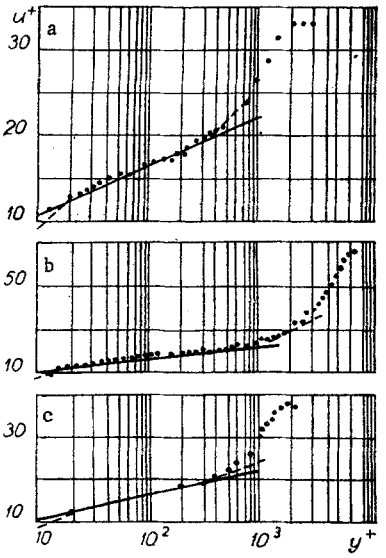

Fig. 1

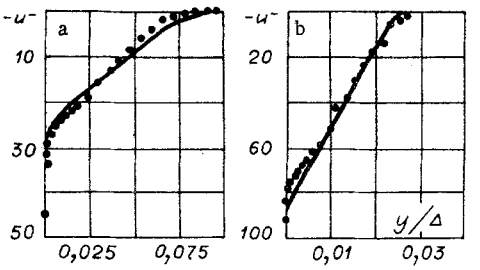

Fig. 2

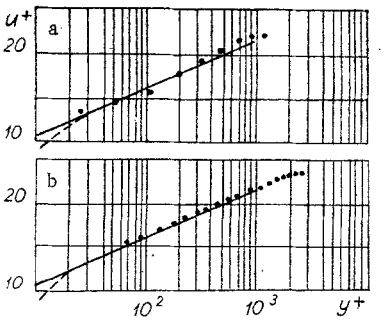

Fig. 3

η_1 is the ordinate at which the velocity defect and overlap zones are separated. The ordinate η_1 at which the velocity profiles from the defect (2.14) and the overlap (2.13) zones join was determined from the condition $l(\tau_+^{1/2})\ /\varkappa\Delta_1 = \alpha_1$. For gradient-free flows, for the values of $\alpha_1 = 1$ and $\Delta_1 = 3.875$ [18], we find $\eta_1 = 0.2$. If we take $\alpha_1 = 0.72$ and $\Delta_1 = 3.785$, then we obtain $\eta_1 = 0.15$. Both these values of η_1 are in the interval of standard values [2, 16, 22]. However, the logarithmic velocity distribution (2.6) starts to deviate from the experimental for values of η_1 exceeding 0.15 [16]. Therefore, $\eta_1 = 0.15$ can be considered as the approximate boundary between the near-wall and the outer regions [16]. The overlap zone should not emerge beyond the scope of the near-wall region, and hence the value $\eta_1 = 0.15$ is taken as the ordinate where the velocity profiles of the defect and overlap zones join. In the case of the presence of a positive pressure gradient, the coefficients $\varkappa$ and α_1 depend on the latter. The experiments of the Stanford conference [15] were used to determine the dependences of $\varkappa$ and α_1 on the gradient, as were also numerical experiments on the digital computer Mir-2 using the reduced approximate formulas, and the dependences of other authors [2, 5, 12]. Analysis of the results of computations and comparisons with experiments permitted obtaining approximate dependences in the form

$$\varkappa = \varkappa_R\,[0{,}00905 + 1/(74.6 + (2.4 + \beta)^2)]; \tag{2.15}$$

$$\alpha_1 = 0.0953211/(1 + p^+) + 24{,}090229/(6.21 + \beta)^2, \tag{2.16}$$

where $\varkappa_R$ is the Cebecci [12] correction for small Reynolds number that equals

$$\varkappa_R = \frac{1{,}55}{1 + 0.55\left(1 - e^{-0.243\sqrt{z_1} - 0.298 z_1}\right)},\quad z_1 = \frac{R^{**}}{425} - 1.$$

A comparison of the computed velocity defects (solid line) with experimental results (points) of H. Ludwig and W. Tillman (id. 1200, x = 3.532) – a and G. Schubauer and P. Klebanoff (id. 2100, x = 25.4) – b is shown in Fig. 2. As a result of the computations, it was detected that conservation of values of the coefficients from the gradient-free flows in flows with positive gradient results in growth of the values of η_1 and n. Rotation of the velocity profile around a certain inner point is observed. Values of the velocity grow in absolute magnitude near the wall and diminish near the outer boundary.

3. In the case of flows with negative pressure gradient, the results in Sec. 2 can be used for $\Phi \geq -1$. We hence examine flows with $\Phi < -1$. In the transition and viscous zones $|p^+y^+| < 1$ [15], and hence, the results of Sec. 2 are here again suitable for the velocity distribution. In the wall-law zone, the expression

$$u^+ = \frac{1}{k}\ln\left|\frac{1 - \sqrt{1 - p^+y^+}}{1 + \sqrt{1 - p^+y^+}}\right| + C,$$

$$C = \frac{1 + p^+y_*}{\varkappa_1}\,\mathrm{th}\,(\varkappa_1 y_*) - \frac{p^+}{\varkappa_1^2}\ln[\mathrm{ch}\,(\varkappa_1 y_*)] - \frac{1}{k}\ln\left|\frac{1 - \sqrt{1 - p^+y_*}}{1 + \sqrt{1 - p^+y_*}}\right|.$$

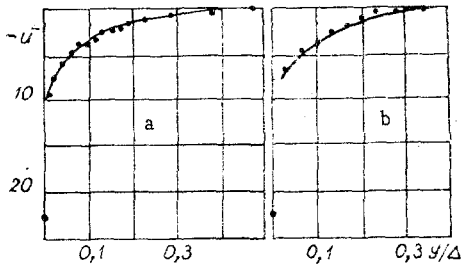

Fig. 4

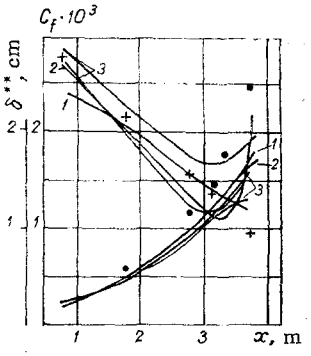

Fig. 5

is obtained for the velocity distribution. The dependence (2.9) is used to calculate y_*. The approach of Sec. 2 and of [17, 18] was used to obtain the velocity distributions in the defect and overlap zones. The following approximations are obtained

$$u^- = \frac{1}{k}\left[\ln\frac{\sqrt{1-\Phi\eta}-1}{\sqrt{1-\Phi\eta}+1} - \frac{2\Phi+1}{(-\Phi-1)^{3/2}}\operatorname{arctg}\left(\sqrt{1-\Phi\eta}\,\sqrt{-\Phi-1}\right) + \right.$$
$$\left. + \frac{\sqrt{1-\Phi\eta}}{1+\Phi}\right] + \frac{1}{\varkappa\Delta_1}\left[\frac{1}{\Phi}\frac{\eta^{n+1}-1}{n+1} - \frac{0.5}{\Phi}\frac{\eta^{n+2}-1}{n+2}\right] + R_1 \quad \text{at} \quad \eta \leqslant \eta_1,$$

$$u^- = \frac{1}{\varkappa\Delta_1}\left[-\frac{\Phi+0.5}{(\Phi+1)^2}\ln\frac{1-(\Phi+1)\eta}{-\Phi} + \frac{0.5(\eta-1)}{\Phi+1} + \frac{1}{\Phi}\left(\frac{\eta^{n+1}-1}{n+1} - 0.5\frac{\eta^{n+2}-1}{n+2}\right)\right] \quad \text{at} \quad \eta \geqslant \eta_1,$$

where

$$\eta_1 = -0.5\left(\alpha_1\frac{\varkappa\Delta_1}{k}\right)^2\Phi + \sqrt{0.25\left(\alpha_1\frac{\varkappa\Delta_1}{k}\right)^4\Phi^2 + \left(\alpha_1\frac{\varkappa\Delta_1}{k}\right)^2};$$

$$R_1 = \frac{1}{k}\left[\ln\frac{\sqrt{1-\Phi\eta_1}+1}{\sqrt{1-\Phi\eta_1}-1} + \frac{2\Phi+1}{(-\Phi-1)^{3/2}}\operatorname{arctg}\left(\sqrt{1-\Phi\eta_1}\,\sqrt{-\Phi-1}\right)\right.$$
$$\left. - \frac{\sqrt{1-\Phi\eta_1}}{\Phi+1}\right] + \frac{1}{\varkappa\Delta_1}\left[\frac{0.5(\eta_1-1)}{\Phi+1} - \frac{\Phi+0.5}{(\Phi+1)^2}\ln\frac{1-(\Phi+1)\eta_1}{-\Phi}\right];$$

$$r = \sqrt{1-\Phi\eta_1};$$

$$n = -2{,}5 - \frac{1}{2F} + \sqrt{\left(2{,}5+\frac{1}{2F}\right)^2 - 6 - \frac{4}{F}}; \quad F = 2\Phi\left(\varkappa\Delta_1^2 + \frac{\varkappa\Delta_1}{k}F_1 + F_2\right);$$

$$F_1 = \frac{2\Phi^2+2\Phi+1}{(\Phi+1)^2}\frac{r-1}{\Phi} - \frac{r\eta_1}{\Phi+1} - \frac{2\Phi+1}{(-\Phi-1)^{5/2}}\operatorname{arctg}\frac{(r-1)\sqrt{-1-\Phi}}{1-(\Phi+1)r} - \frac{2}{3}\frac{r^3-1}{\Phi(\Phi+1)};$$

$$F_2 = -\frac{\Phi+0.5}{(\Phi+1)^3}\ln\frac{1-(\Phi+1)\eta_1}{-\Phi} + \frac{1-\eta_1}{(\Phi+1)^2}(0{,}5+\Phi) + \frac{\eta_1^2-1}{4(\Phi+1)}.$$

Processing the results of computations using the formulas cited, and analysis of the comparisons between computations and experiments [15] show that even for a negative pressure gradient, (2.15), (2.16), (2.11) can be used for $\varkappa$, α_1, and $\varkappa_1$. As regards the coefficient k, (2.10) can be used even to calculate it, but the dependence

$$k = 0{,}4 + 58{,}510275(p^+/\beta)(1 - e^{-0.320688\beta}).$$

results in more successful outcomes.

The comparison between the computed values (dashed line) of u^+ by using the formulas cited and the experimental data of G. Schubauer and P. Klebanoff (id. 2100, x = 1.0) – a, H. Herring and I. Norbury (id. 2800, x = 3) – b is shown in Fig. 3. The wall law (2.6) is shown for k = 0.41 and C = 5.0 [15] by the solid line. It is seen from the comparison that (2.6) with constant coefficients can be used in the wall-law zone with sufficient accuracy for practice. The computed values by using the mentioned formulas practically coincide in the wall-law zone.

Computed values of the velocity defect (dashes) u^- and experiment (points) of H. Ludwig and W. Tillman (id. 1300, x = 2.282) – a, and I. Bell (id. 3100, x = 2.041) – b [15] are compared in Fig. 4. The comparison between the computed and test values shows that for a negative pressure gradient [15] satisfactory results for the velocity defect can be obtained both with and without taking into account the corrections to the coefficients $\varkappa$ and k for small Reynolds number and for a gradient. The discrepancies between the numerical values of

the computations are not outside the limits of the spread in the experimental results. Experiment and computed values are compared in Fig. 4a with the mentioned corrections taken into account, and in Fig. 4b without taking the corrections into account. Computations in the velocity defect for both a negative and a positive gradient showed that the profiles are responsive to a change in and selection of the value of the outer boundary of the boundary layer δ.

Shown in Fig. 5 is the comparison between the computed values (curve 1) by the method of lines by using (1.1) and (1.2) without taking account of the corrections and the experiment of H. Ludwig and W. Tillman (id. 1200) for the friction coefficient c_f (crosses) and the thickness of the loss of momentum δ^{**} (points), as well as computations from [3] (curve 2) and [13] (curve 3). The computation shows the absence of sharp deviations from experiment for a significant unfavorable gradient.

LITERATURE CITED

1. G. V. Kocheryzhnikov and S. K. Matveev, "On a test of numerical integration of a turbulent boundary layer," in: Hydromechanics and Elasticity Theory [in Russian], No. 13 (1968).
2. S. J. Kline, M. V. Morkovin, G. Sovran, and G. J. S. Cockrell (eds.), "Computation of turbulent boundary layers," 1968 AFOSR-IFP-Stanford Conference, Vol. 1 (1969).
3. K. K. Fedyaevskii, A. S. Ginevskii, and A. V. Kolesnikov, Computation of the Incompressible Fluid Turbulent Boundary Layer [in Russian], Sudostroenie, Leningrad (1973).
4. V. N. Dolgov and V. M. Shulemovich, "Turbulent viscosity for incompressible gradient flows in preseparation regions and on a rough surface," Zh. Prikl. Mekh. Tekh. Fiz., No. 3 (1977).
5. Horstman, "Turbulence model for the computation of nonequilibrium flows with a positive pressure gradient," Raket. Tekh. Kosmon., 15, No. 2 (1977) (AIAA J.).
6. Pletcher, "Computations of incompressible turbulent separation flow," Teor. Osnovy Inzh. Raschetov, No. 4 (1978).
7. J. C. Cheng, W. L. Hankin, and J. S. Petti, "Three-dimensional supersonic turbulent flow within a dihedral angle," Raket. Tekh. Kosmn., No. 7 (1977) (AIAA J.).
8. V. T. Movchan and B. D. Zakharyugin, "Computation of the turbulent boundary layer on a flat plate by the method of lines," Gidromekhanika, No. 40 (1979).
9. V. T. Movchan and B. D. Zakharyugin, "Computation of the turbulent boundary layer on the basis of a single representation of the turbulent viscosity across the boundary layer," Prikl. Aerodinamika (1979).
10. D. R. Chapman, "Computational aerodynamics and prospects for its development," Raket. Tekh. Kosmon., 18, No. 2 (1980).
11. P. Bradshaw (ed.), Turbulence [Russian translation], Mashinostroenie, Moscow (1980).
12. Cebecci and Mosinskis, "Computation of the incompressible turbulent boundary layer for small Reynolds numbers," Raket. Tekhn. Kosmon., 9, No. 8 (1971) (AIAA J.).
13. V. V. Novozhilov, Theory of the Plane Turbulent Incompressible Fluid Boundary Layer [in Russian], Sudostroenie, Leningrad (1977).
14. Yu. V. Lapin and A. L. Yarin, "Problem of 'merger' in the theory of nonequilibrium turbulent flows," Izv. Akad. Nauk SSSR, Mekh. Zhidk. Gaza, No. 3 (1979).
15. D. E. Coles and E. A. S. Hirst (eds.), Computation of Turbulent Boundary Layers. 1968 AFOSR-IFP-Stanford Conference, Vol. 2 (1969).
16. J. O. Hinze, Turbulence, McGraw-Hill (1975).
17. V. T. Movchan, "Approximate method of calculating the friction stress and velocity profiles in a turbulent flow with positive pressure gradient," Gidromekhanika, No. 26 (1975).
18. V. T. Movchan, "On the investigation of turbulent flows," in: Stratified and Turbulent Flows [in Russian] (1979).
19. V. T. Movchan, "On the calculation of the turbulent viscosity coefficient," Gidromekhanika, No. 41 (1980).
20. B. D. Kadr and A. M. Yaglom, "Mean velocity profiles and drag laws in turbulent boundary layers with decelerating pressure gradient," in: Mechanics of Turbulent Flows [in Russian], Nauka, Moscow (1980).
21. H. McDonald, "The effect of a pressure gradient on the law of the wall in turbulent flow," J. Fluid Mech., 35, No. 2 (1969).
22. S. S. Kutateladze, "Three problems of the theory of heat transfer and physical hydrogasdynamics," Inzh.-Fiz. Zh., 39, No. 6 (1980).
23. S. S. Kutateladze, B. P. Mironov, V. E. Nakoryakov, and E. M. Khabakhpasheva, Experimental Investigation of Near-Wall Turbulent Flows [in Russian], Nauka, Novosibirsk (1975).